Radiotherapy and Oncology 144 (2020) 224–230

Contents lists available at ScienceDirect

Radiotherapy and Oncology

journal homepage: www.thegreenjournal.com

Original Article

Dose assessment for patients with stage I non-small cell lung cancer receiving passive scattering carbon-ion radiotherapy using daily computed tomographic images: A prospective study

Yang Li [a,b], Yoshiki Kubota [c,*], Nobuteru Kubo [c], Tatsuji Mizukami [c], Makoto Sakai [c], Hidemasa Kawamura [c], Daisuke Irie [c], Naoko Okano [c], Kazuhisa Tsuda [d], Akihiko Matsumura [c], Jun-ichi Saitoh [e], Takashi Nakano [c], Tatsuya Ohno [c]

[a] Graduate School of Medicine, Gunma University, Japan; [b] Department of Breast Radiotherapy, Harbin Medical University Cancer Hospital, China; [c] Gunma University Heavy Ion Medical Center; [d] Department of Radiology, Gunma University Hospital; and [e] Department of Radiation Oncology, Faculty of Medicine, University of Toyama, Japan

ARTICLE INFO

Article history:
Received 20 June 2019
Received in revised form 10 December 2019
Accepted 2 January 2020

Keywords:
Carbon-ion radiotherapy
Dose assessment
Tumor matching
Bone matching
Lung cancer

ABSTRACT

Background and purpose: This study aimed to assess dose distributions for stage I non-small cell lung cancer (NSCLC) with passive scattering carbon-ion radiotherapy (C-ion RT) using daily computed tomography (CT) images.

Materials and methods: We enrolled 10 patients with stage I NSCLC and acquired a total of 40 pre-fractional CT image series under the same settings as the planning CT images. These CT images were registered with planning CT images for dose evaluation using both bone matching (BM) and tumor matching (TM). Using deformable image registration, we generated accumulated doses. Moreover, the volumetric dose parameters were compared in terms of tumor coverage and lung exposure and statistical analyses were performed.

Results: Overall, 25% of 40 fractional dose distributions were unacceptable with BM, compared with 2.5% with TM ($P < 0.001$). Using BM, three patients' accumulated dose distributions were unacceptable; however, all were satisfactory with TM ($P < 0.001$). No differences were observed in water-equivalent path length (WEL). The required margins in patients with poor dose distribution were 5.9 and 4.4 mm for BM and TM, respectively.

Conclusions: This study establishes that CT image-based TM is robust compared with conventional BM for both daily and accumulated dose distributions. The effects of changes in WEL seem to be limited. Hence, daily CT alignment is recommended for patients with stage I NSCLC receiving C-ion RT.

For over two decades now, carbon-ion radiotherapy (C-ion RT) has been used for the treatment of early-stage non-small cell lung cancer (NSCLC) [1]. Compared with stereotactic body radiotherapy, which has exhibited promising outcomes for inoperable early-stage NSCLC [2], C-ion RT facilitates delivering a higher dose to the target with extremely low lung toxicity because of its fine dose concentration [3,4]. These advantages make C-ion RT a good treatment option for patients with NSCLC. However, C-ion RT is highly sensitive to anatomical changes that merit focus, especially for mobile tumors. Dose degradation caused by tumor movement is regarded as one of the potential factors for local recurrence in patients with NSCLC [5,6].

The gated computed tomography (CT) and four-dimensional CT (4DCT) have been routinely used to manage the tumor motion [7]. The effects of respiratory motion are limited when an appropriate internal margin is applied [8]. However, the interfractional anatomical changes are the main source of the dose degradation in C-ion RT. Most published studies focus on their effects on the particle dose in a conventional treatment schedule (5–6 weeks) for patients with lung cancer using limited CT scans or 2D imaging technology [6,9–11]. However, very few studies report hypofractionated C-ion RT. Recently, tumor displacement and changes in water-equivalent path length (WEL) have been reported to be significant influencing factors for dose degradation in hypofractionated particle therapy, and tumor matching (TM) was found to

* Corresponding author at: Gunma University Heavy Ion Medical Center, 3-39-22, Showa-machi, Maebashi, Gunma 371-8511, Japan.
E-mail addresses: dr.yang.li@foxmail.com (Y. Li), y_kubota@gunma-u.ac.jp (Y. Kubota), kubo0330@gmail.com (N. Kubo), tmizukam36@gmail.com (T. Mizukami), sakai-m@gunma-u.ac.jp (M. Sakai), kawa@gunma-u.ac.jp (H. Kawamura), i_want_ my_hero@hotmail.co.jp (D. Irie), naokomaezawa@hotmail.co.jp (N. Okano), ktsuda@gunma-u.ac.jp (K. Tsuda), matchan.akihiko@gunma-u.ac.jp (A. Matsumura), junsaito@med.u-toyama.ac.jp (J.-i. Saitoh), tnakano@gunma-u.ac.jp (T. Nakano), tohno@gunma-u.ac.jp (T. Ohno).

https://doi.org/10.1016/j.radonc.2020.01.003
0167-8140/

ensure better dose distribution than bone matching (BM) in daily dose distributions [12–14]. However, the effects of these uncertainties on the accumulated dose are still unclear. Considering that a poorly accumulated dose may lead to failure of treatment, evaluation of the accumulated dose is crucial in routine clinical practice. Several studies have investigated the accumulated dose in particle RT for pancreatic and liver cancer using daily CT images [15,16]. However, to the best of our knowledge, there has been no such report for stage I lung cancer with hypofractionated C-ion RT.

Therefore, this prospective study aimed to investigate the daily dose changes and accumulated dose in patients with stage I NSCLC using actual daily in-room CT images, as well as BM and TM positioning methods for comparison.

Methods and materials

Study design and patient selection

We prospectively examined ten consecutive patients with stage I NSCLC, between June 2017 and November 2018, who were treated with C-ion RT using passive irradiation methods at our center. Table 1 summarizes the patient-specific clinical data. This study protocol was approved by the Institutional Review Board of Gunma University Hospital and was registered at the University Hospital Medical Information Network Clinical Trials Registry (UMIN-CTR trial number: 000027125).

Image acquisition

We acquired respiratory-gated CT images for treatment planning around the maximum expiration using a multislice CT system (Aquilion LB; Canon Medical Systems, Japan). Then, we performed a 4DCT scan to quantify the respiratory motion during 30% respiration phase. In actual treatment, the same gating window was adopted for respiratory-gated irradiation [7]. Patients were immobilized in either supine or prone postures with a customized patient pillow (Moldcare; ALCARE, Japan) and a body shell (Shellfitter; Sanyo Polymer Industrial, Japan). Patients were rolled ±15° (except for patient 2: 0° and −15° were used) around the superior–inferior axis for oblique beam irradiation. Two planning CT image series of two body positions were acquired. We acquired daily gated-CT images around the end of exhalation on each treatment day using a self-propelled CT scanner on rails in a treatment room. In our center, TM is applied when the tumor displacement is larger than 3 mm or the amplitude of the diaphragm is larger than 10 mm. To avoid potential uncertainties between the day of planning CT acquisition and the first treatment delivery (approximately 1–2 weeks), CT images taken on the first treatment day were used as reference CT (ref-CT) for dose accumulations. In total, 40 daily CT images were obtained.

Treatment planning

The gross target volume (GTV) was delineated on planning CT in the lung window; the clinical target volume (CTV) was defined as the GTV plus a 5-mm margin in all directions. The internal margin (IM) was calculated by adding one-third of tumor motion in each direction. In addition, the planning target volume (PTV) was generated by anisotropically adding a total margin to CTV, which was calculated using the IM and 3 mm of setup margin (SM) [7]:

$$Total\ margin = \sqrt{(IM)^2 + (SM)^2} \quad (1)$$

To compensate the changes of the WEL in each direction, two-thirds of the total margin in the forward and backward directions against the beam were set as the proximal and distal margin. The maximum value of the total margins perpendicular to the beam axis was used for the smearing to compensate the change of range accompanied by motion. We performed treatment planning using a XiO-N system that employs a pencil beam algorithm (collaborated product of Elekta AB, Stockholm, and Mitsubishi Electric, Japan) [17]. We used Gy (RBE) as the unit of the clinical dose, which was calculated based on the physical dose and the relative biological effectiveness (RBE) [18]. The prescribed dose was 60 Gy (RBE) in four fractions. The isocenter doses become the prescribed dose after dose calculation in the XiO-N, and PTV must be covered by 95% of the prescribed dose in the treatment plan. Each fraction comprised the vertical and horizontal ports with +15° or −15° (0° and −15° for patient 2) of the body roll. Therefore, a total of four directions were used to ensure a satisfactory dose distribution.

Image matching and accumulated dose calculation

Firstly, rigid image registration between daily CT and planning CT were performed by referring to the bone structure using MIM Maestro (ver. 6.8; MIM Software, OH). Then, we manually matched spinal bones and tumors for BM and TM, respectively. Matching corrections were performed by experienced radiation oncologists. After matching the images, daily CT images with contours (PTV) were transferred to the XiO-N system for calculation using the same parameters as those of the original treatment plan. Next, daily CT images acquired on the second, third and fourth treatment day were registered into ref-CT images using deformable image registration (DIR). Furthermore, three warped dose distributions were generated using the respective deformation matrices; these warped dose distributions and the dose distribution for the ref-CT images were accumulated. More details are available in Fig. 1.

Table 1
Patient characteristics.

Patient No.	Sex	Age (year)	BMI	Emphysema or COPD	Tumor location	Tumor Volume (cm^3)	Treatment position	Tumor motion (mm)					
								R	L	A	P	S	I
1	F	82	22.89	None	L + SL (S′3)	7.43	SP	0	2	0	1	0	2
2	F	88	22.16	None	R + IL (S′6)	5.89	PR	0	1	0	1	0	2
3	M	80	21.83	Yes	L + SL (S′1 + 2)	12.51	PR	1	1	2	1	3	4
4	M	69	25.35	Yes	R + IL (S′6)	4.5	PR	1	0	2	0	0	2
5	F	87	17.95	None	L + IL (S′6)	1.9	PR	1	0	1	0	1	2
6	M	72	30.43	None	L + SL (S′1 + 2)	36.73	PR	1	0	1	0	2	0
7	M	71	25.22	Yes	L + IL (S′10)	2.04	PR	2	1	1	0	1	8
8	M	84	19.38	None	L + SL (S′4)	10.86	SP	0	0	0	0	0	2
9	M	77	21.99	Yes	L + SL (S′3)	1.7	SP	0	1	0	1	0	0
10	M	79	23.56	None	L + SL (S′2)	16.55	PR	2	0	1	0	1	0

F, female; M, male; BMI, Body Mass Index; COPD, chronic obstructive pulmonary disease; PTV, planning target volume; L, left; R, right; A, anterior; P, posterior; S, superior; I, inferior; SL, superior lobe; IL, inferior lobe; S ‘, segments; SP, supine; PR, prone.

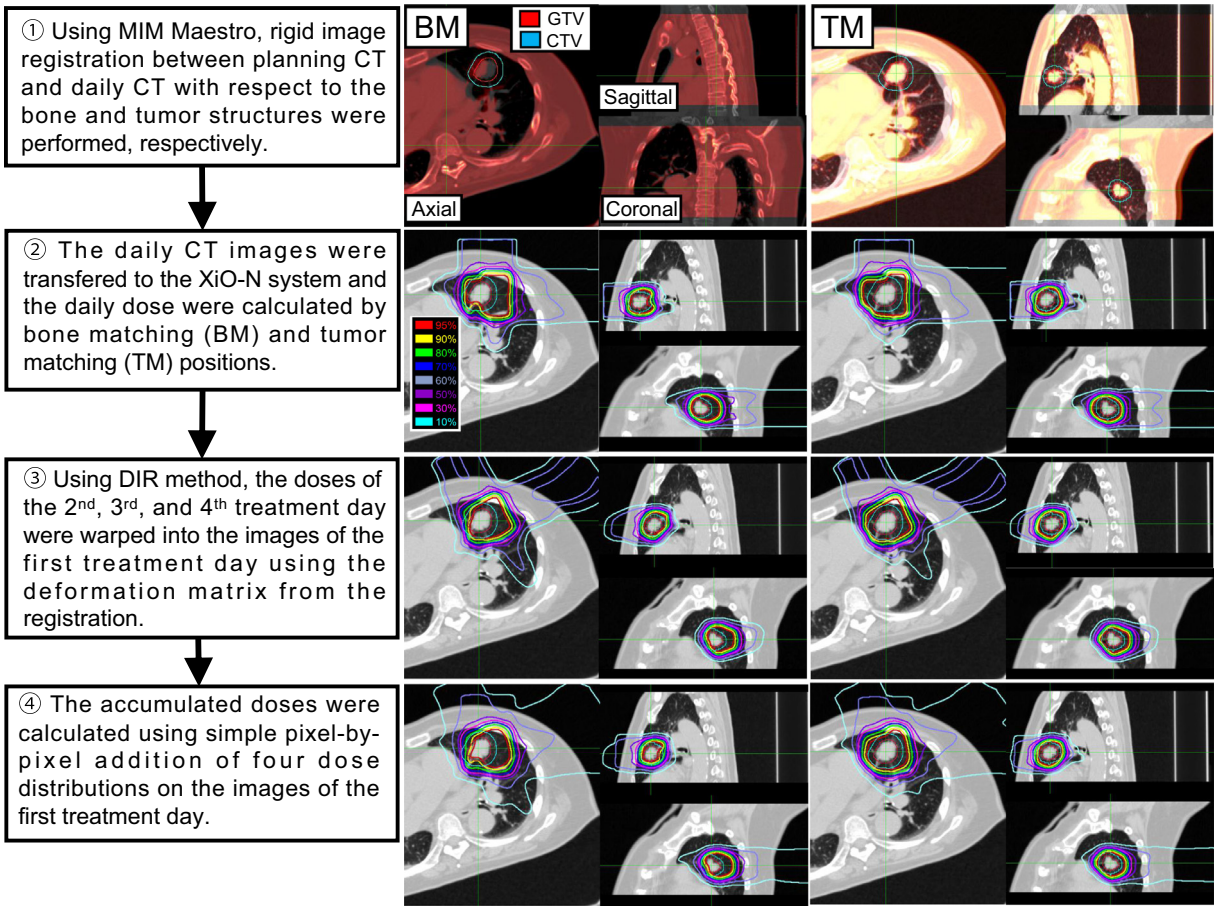

Fig. 1. The flow chart of image matching and the dose calculations. CT images are shown in axial, coronal, and sagittal planes. The left and right panels show the CT images (patient 1) with BM and TM, respectively. The images of the first treatment day were used as an example in the first and second steps; doses of the second treatment day were deformally transferred in the third step. The GTV, CTV and isodose lines are also displayed. BM, bone matching; TM, tumor matching; GTV, gross tumor volume; CTV, clinical target volume.

Statistical analysis

We measured the tumor displacement in three directions, left–right (LR), anterior–posterior (AP), and superior–inferior (SI), and evaluated it as the displacement of the center of GTV on each image after registration with BM using planning CT and daily CT images. In addition, the absolute tumor displacement (*ATD*) and relative tumor displacement (*RTD*) were used to evaluate the correlation between the target coverage and tumor movement. *ATD* and *RTD* were defined as follows:

$$ATD = \sqrt{T_x^2 + T_Y^2 + T_z^2} \tag{2}$$

where $T_{x,y,z}$ is defined as the tumor movement between the planning CT and daily CT images on the *x*-, *y*-, and *z*-axes.

$$RTD = ATD - \sqrt{P_x^2 + P_y^2 + P_z^2} \tag{3}$$

where $P_{x,y,z}$ is defined as the margin from the CTV to the PTV on the *x*-, *y*-, and *z*-axes.

We evaluated the parameters of the dose-voslume histogram (DVH), such as the percentage of the CTV receiving ≥95% of the prescription dose (V95) and the minimum doses covering 98%, 95%, and 90% of the CTV (D98, D95, and D90). We defined unacceptable cases as those with CTV V95 <95%. To assess toxicity, we evaluated the percentage of the total lung volume receiving ≥20 Gy (RBE) and 5 Gy (RBE) (V20 and V5, respectively).

We gradually added an isotropic margin to the CTV by 1 mm and reevaluated the dose on all daily CT images using treatment plans to compare the robustness of two positioning methods. Thus, the required margins for daily and accumulated dose were obtained (intrafractional tumor motion were not considered). The curve fitting of sigmoid functions was used to ascertain the required margin, which enabled 95% of cases to attain an acceptable condition. We used the Wilcoxon and Friedman tests to compare the parameters of DVH and accumulated dose. Moreover, the Kruskal–Wallis test was used to analyze the tumor displacement. In this study, we considered $P < 0.05$ as statistically significant.

Results

Compared with LR and AP directions, the SI direction exhibited the highest displacement amplitude ($P < 0.05$; Supplementary Fig. 1). The dose conformality with BM negatively correlated with the tumor displacement (Fig. 2). We obtained a better correlation coefficient when *RTD* was used ($R = -0.73$ vs. $R = -0.89$). TM enables much better accumulated doses and fractional doses than BM ($P < 0.001$) (Table 2); no statistical difference was noted in WEL changes. Only one fractional dose in TM was not satisfactory because of large changes in WEL (8 mm). TM also enabled a better accumulated dose in D98, D95, and D90 than BM ($P < 0.05$) (Table 3). No significant difference was noted in lung V20 and V5.

The V95 and acceptance ratio for BM and TM evaluated after isotropic margins were applied (Fig. 3). We obtained a significant

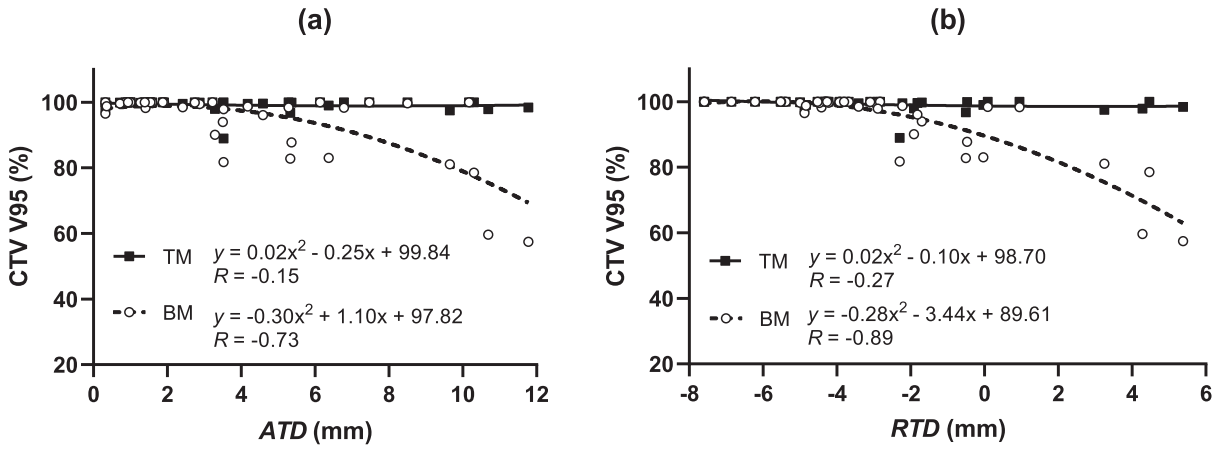

Fig. 2. Dependence of fractional V95 on the *ATD* (a) and *RTD* (b).

Table 2
Dose distributions through the entire course of treatment.

Patient No.	Tumor displacement (mm)	WEL changes (mm)		Daily dose distribution (CTV V95 (%))		Acceptance ratio (%)		Accumulated dose (CTV V95 (%))		
		BM	TM	BM	TM	BM	TM	Plan	BM	TM
1	10.2 (6.4–11.8)	3.8 (−7.4 to 9.1)	−0.9 (−3.8 to 2.9)	70.4 (57.5–83.1)	98.2 (97.5–99)	0	100	96.2	60.6	95.6
2	3.4 (0.3–5.3)	−1.3 (−10.3 to 2.9)	−2.8 (−8 to 1.6)	88.8 (82.8–96.6)	97.4 (88.9–98.3)	25	75	98.2	88.1	95.4
3	1.3 (1–3.2)	0.3 (−5 to 2.3)	1.2 (−2.6 to 3.5)	100 (100–100)	100 (100–100)	100	100	100	100	100
4	1.7 (1.4–5.3)	2.4 (−0.6 to 5)	−0.3 (−4.2 to 3.1)	99.2 (98.3–100)	100 (100–100)	100	100	100	99.6	100
5	2.0 (0.8–2.9)	−2.9 (−6.5 to 0.6)	−1.4 (−2.5 to 0.7)	99.6 (98.5–100)	99.9 (99.5–100)	100	100	100	99.9	99.9
6	0.6 (0.3–3.5)	−3.4 (−6.1 to 2.1)	−2.6 (−4.1 to 1.8)	99.4 (94.0–100)	99.9 (99–100)	75	100	100	99.3	100
7	8.0 (6.1–10.2)	0.6 (−1.9 to 5.2)	−1.6 (−2.5 to 3.3)	100 (99.7–100)	100 (100–100)	100	100	100	99.9	100
8	6.1 (2.7–10.3)	−0.5 (−1.4 to 4.7)	0.2 (−2.9 to 2.1)	93.1 (78.5–99.9)	100 (99.9–100)	50	100	100	85.2	99.1
9	1.1 (0.7–1.4)	−1.6 (−4.3 to 2.6)	−0.4 (−2.2 to 2.1)	99.9 (99.6–100)	100 (99.9–100)	100	100	100	99.9	100
10	3.9 (1.9–4.6)	0.6 (−12.5 to 2.2)	1.5 (−5.1 to 7.7)	98.3 (96.1–100)	99.8 (99.6–100)	100	100	100	99.4	100
Total	3.1 (0.3–11.8)	−0.6 (−12.5 to 9.1)	−0.9 (−8 to 7.7)	99.5 (57.5–100)*	100 (88.9–100)	75	97.5	100 (96.2–100)	99.5 (60.6–100)*,†	100 (95.6–100)

Data are presented as median (range). BM, bone matching; TM, tumor matching; CTV, clinical target volume; V95, percentage of target volume that included 95% of the prescribed dose area; WEL, water-equivalent path length.
*$P < 0.05$ compared with TM; †$P < 0.05$ compared with plan.

Table 3
Dose-volume histogram parameters of accumulated dose.

Object	Parameter	Plan	BM	TM	*P* value
CTV	D98 (Gy (RBE))	59.3 (55.8–59.7)	58.1 (41.3–59.7)*	58.9 (56.1–59.8)	<0.001
	D95 (Gy (RBE))	59.5 (57.5–59.9)	58.7 (45.9–59.8)*	59.2 (57.1–59.8)	<0.001
	D90 (Gy (RBE))	59.6 (58.5–60)	59.1 (50–59.8)*	59.4 (57.8–59.9)	0.003
Lung	V5 (%)	10.9 (4.6–18.2)	11 (4.3–18.7)	10.7 (4.5–18.8)	0.973
	V20 (%)	6.5 (2.1–10.9)	6.3 (1.8–11)	6.4 (1.9–11)	0.590

Data are presented as median (range). BM, bone matching; TM, tumor matching; CTV, clinical target volume; D90, D95, and D98, minimum doses covering 90%, 95%, or 98% of the clinical target volume; V5 and V20, percentage of the total lung volume receiving ≥20 Gy (RBE) and 5 Gy (RBE). *$P < 0.05$ compared with plan and TM.

difference for the entire margin between BM and TM ($P < 0.001$). To make 95% of patients exceed the acceptable condition, the required margins for accumulated and daily dose between BM and TM were 5.9 and 4.4 mm and 6.6 and 4.5 mm, respectively. For acceptable cases, TM enabled a better dose coverage with tight margins (1–4 mm) than BM ($P < 0.05$), and the required margins for accumulated and daily dose were close: 2.9 and 3 mm in TM and 4 and 4.1 mm in BM.

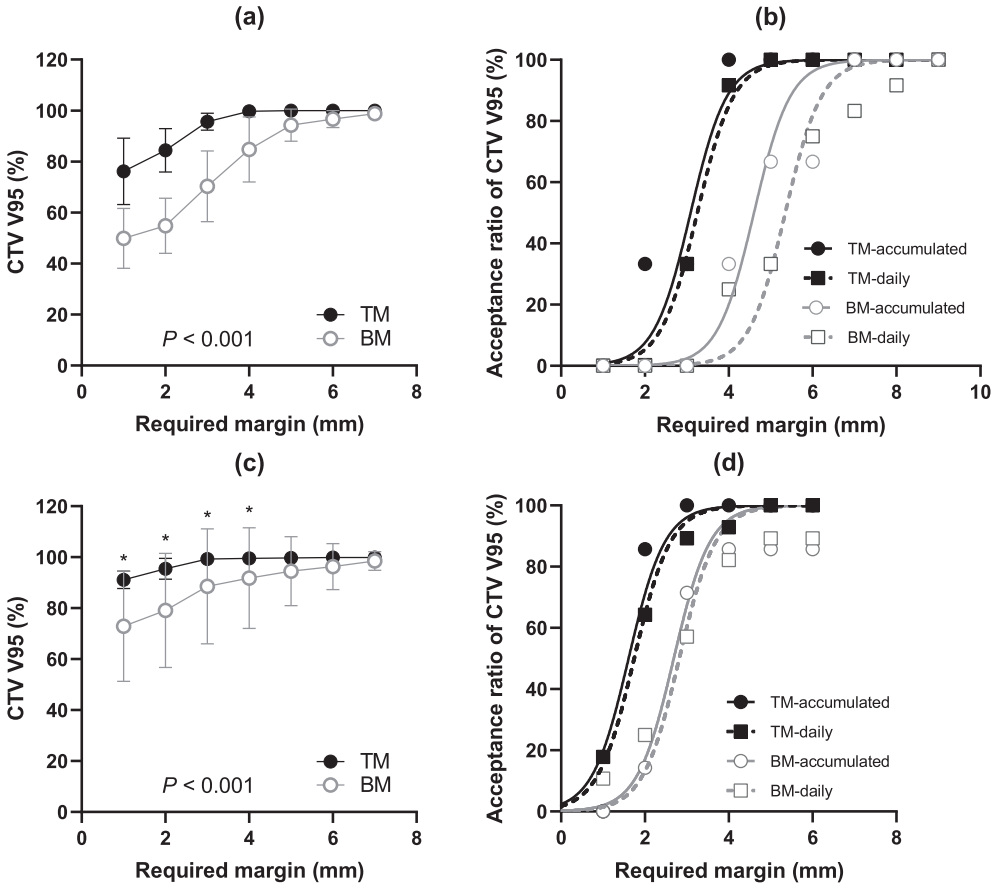

Fig. 3. Relationship between CTV V95 (%) of accumulated dose and required margin and acceptance ratio of CTV V95 (%) for unacceptable cases (a, b) and acceptable cases (c, d). *P < 0.05. The required margin was proposed to compensate the interfractional deviations; the respiratory movement was not taken into consideration.

Discussion

The hypofractionated C-ion RT has been widely adopted as a more efficient treatment strategy. A few-fraction proposal needs an evaluation of the daily dose for ensuring successful treatment. Although CT image-guidance has been routinely applied in photon RT [19], in-room 3D imaging is not a standard method in particle therapy [20]. The direct evidence is very limited, especially for the study based on data representative of the whole course of treatment.

Corroborating prior studies [12,13], we observed large interfractional displacements in all directions in this study. The tumor displacement negatively correlated with the dose distribution (Fig. 2); although it does not show strong dependence in Fig. 2a, the trend is apparent, especially when *RTD* was applied (Fig. 2b). Although a majority of treatment fractions had a relatively small tumor displacement, our findings revealed that these deviations should be considered in clinical practice because of their irregularity during treatment (Table 2). As varied acceptance ratio suggests more uncertainties in BM, the interfractional tumor movement remains a problem for C-ion RT centers using 2D imaging system. However, WEL changes should also be considered carefully after TM, which may degrade the dose. Unfortunately, we could not calculate a cutoff value because of our small sample size. Irie et al. [12] suggested 5.4 mm of the chest wall thickness as the cutoff value for WEL changes; however, it was obtained by using BM where its reliability may decline when large tumor displacement happens (tumor moves out of the radiation field). Therefore, offline verification seems essential for TM, and replanning is recommended to address this problem. Furthermore, the tumor volume was not a factor affecting WEL in this study because its change was minimal over the entire treatment.

Although a study highlighted that there is no correlation between respiratory movement and the interfractional tumor displacement [12], we found that the amplitude of tumor respiratory movement may be positively correlated to the mean interfractional tumor displacement in SI direction (R = 0.86) (Supplementary Fig. 2). This indicates that large interfractional deviations may occur in patients (especially for the tumor in the lower lobes of the lungs) who have a large respiratory movement; therefore, such patients merit special attention. However, it seemed more complicated for tumors in the upper lobes of the lung. For patients 1 and 8, large interfrcactional tumor displacements occurred in all directions among fractions; the irregularity of these deviations makes it difficult to determine a specific cause. Presently, markerless tumor tracking technology combined with C-ion RT is applied to monitor daily tumor movement [11]; however, it is a prediction method using the templates and machine learning dictionary files, which does not capture the tumor position directly. Reportedly, the voluntary breath-hold method, combined with TM, helps ensure the interfractional reproducibility of the lung tumor location [21]. However, other measurements, such as abdominal compression, are not recommended, which may cause increased interfractional variations [22].

Low radiation dose is a critical factor for tumor recurrence of NSCLC [23,24]. Therefore, we evaluated the accumulated dose for all patients in this study. The three patients' accumulated doses were unacceptable because of tumor displacement (Table 2 and 3). This indicates that using BM may lead to treatment failure. Although some studies have shown similar results based on

1-day CT images [12,13], dose assessment for the entire course of the treatment appears more meaningful. For example, BM enabled an acceptable CTV V95 in 1 day (96.6%), but CTV V95 of the accumulated dose was unacceptable (88.8%; patient 2 in Table 2). TM may also present such uncertainties, suggesting that confirming 1-day dose distribution is not adequate to assess the accuracy of the irradiation, and it is important to obtain the accumulated dose based on all treatment days.

We proposed an isotropic margin to compare the robustness between BM and TM (Fig. 3). TM enables smaller margins than BM, especially in unacceptable cases. Interestingly, ensuring satisfactory accumulated doses need smaller margins than those for daily dose (e.g., 5.9 mm vs. 6.6 mm, BM), which suggests that an excessive margin may be applied when using the margins based on daily dose. Even a 7.9-mm margin based on 1-day CT images was required in another study [13]. Therefore, evaluating the required margins based on the accumulated dose is important because an overestimated margin may lead to unnecessary irradiation to healthy tissues. Promisingly, almost the same size margins were obtained in TM between accumulated and daily dose. TM may provide a safer margin to maintain the robustness of accumulated dose while ensuring a better daily dose. However, compared with acceptable cases, the required margin for accumulated dose was larger (2.9 mm vs. 4 mm) in unacceptable cases. The main cause may be the larger WEL changes and the limited number of patients included in the unacceptable group (Supplementary Table 1). Therefore, further studies are warranted to validate our results.

This study has some limitations. First, the sample size was small. Second, we did not consider the intrafractional changes, such as tumor respiratory motion during treatment, which also affected the dose distribution [25]. A 4D treatment plan based on daily 4DCT or real-time tumor tracking is a promising method to reduce these uncertainties, which have been recently discussed in particle RT [26–28]; moreover, the DIR method has its own uncertainties, although the dose warping errors are generally less than 3% [29,30]. Furthermore, a larger margin may be required to compensate for the interfractional deviations in BM while employing a scanning pencil beam technology; consequently, the effects induced by the changes in the WEL may be greater than those observed in the present study. However, these effects seem to be limited. This is because the differences in the WEL changes between BM and TM were small in this study (Table 2). In addition, compared with the improved target coverage in TM, especially for large tumor displacement, the effects of WEL changes (mainly from the ribs) seem relatively small. However, because of the interplay effects, the scanning method is less robust than passive irradiation technology. This effect seems to be limited in cases where the amplitude of the tumor motion was less than 3 mm [31] or when using the (phase-controlled) rescanning technology [32]. A slight modification in the advantages of TM is expected even when using a scanning beam technology. However, a comparative analysis is necessary, which will be conducted in a subsequent study. Finally, adaptive radiotherapy is recommended for both irradiation methods for few cases with poor dose distributions after TM.

This prospective study estimated the daily and accumulated doses for patients with NSCLC. The varied daily doses make it important to evaluate the accumulated dose. Confirming just 1-day dose is not adequate. The required margins based on accumulated dose proposed in this study are helpful to improve the dose coverage in BM; however, those based on daily dose are not recommended. Compared with BM by the current 2D X-ray imaging system, TM by volumetric images enables a significantly better dose coverage. Although, changes in WEL after TM merit attention, these effects seem limited. Overall, this study recommends in-room CT images for daily alignment and dose assessment for patients with NSCLC with hypofractionated C-ion RT.

Conflict of interest

None.

Funding

This research received no external funding.

Appendix A. Supplementary data

Supplementary data to this article can be found online at https://doi.org/10.1016/j.radonc.2020.01.003.

References

[1] Mohamad O, Makishima H, Kamada T. Evolution of carbon ion radiotherapy at the National Institute of Radiological Sciences in Japan. Cancers 2018;10:66.
[2] Sun B, Brooks ED, Komaki RU, et al. 7-year follow-up after stereotactic ablative radiotherapy for patients with stage I non-small cell lung cancer: results of a phase 2 clinical trial. Cancer 2017;123:3031–9.
[3] Miyamoto T, Baba M, Sugane T, et al. Carbon ion radiotherapy for stage I non-small cell lung cancer using a regimen of four fractions during 1 week. J Thorac Oncol 2007;2:916–26.
[4] Yamamoto N, Miyamoto T, Nakajima M, et al. A dose escalation clinical trial of single-fraction carbon ion radiotherapy for peripheral stage I non-small cell lung cancer. J Thorac Oncol 2017;12:673–80.
[5] Koto M, Miyamoto T, Yamamoto N, et al. Local control and recurrence of stage I non-small cell lung cancer after carbon ion radiotherapy. Radiother Oncol 2004;71:147–56.
[6] Hui Z, Zhang X, Starkschall G, et al. Effects of interfractional motion and anatomic changes on proton therapy dose distribution in lung cancer. Int J Radiat Oncol Biol Phys 2008;72:1385–95.
[7] Tashiro M, Ishii T, Koya J, et al. Technical approach to individualized respiratory-gated carbon-ion therapy for mobile organs. Radiol Phys Technol 2013;6:356–66.
[8] Matney J, Park PC, Bluett J, et al. Effects of respiratory motion on passively scattered proton therapy versus intensity modulated photon therapy for stage III lung cancer: are proton plans more sensitive to breathing motion?. Int J Radiat Oncol Biol Phys 2013;87:576–82.
[9] Koay EJ, Lege D, Mohan R, et al. Adaptive/nonadaptive proton radiation planning and outcomes in a phase II trial for locally advanced non-small cell lung cancer. Int J Radiat Oncol Biol Phys 2012;84:1093–100.
[10] Li H, Zhang X, Park P, et al. Robust optimization in intensity-modulated proton therapy to account for anatomy changes in lung cancer patients. Radiother Oncol 2015;114:367–72.
[11] Mori S, Karube M, Shirai T, et al. Carbon-ion pencil beam scanning treatment with gated markerless tumor tracking: an analysis of positional accuracy. Int J Radiat Oncol Biol Phys 2016;95:258–66.
[12] Irie D, Saitoh JI, Shirai K, et al. Verification of dose distribution in carbon ion radiotherapy for stage I lung cancer. Int J Radiat Oncol Biol Phys 2016;96:1117–23.
[13] Sakai M, Kubota Y, Saitoh JI, et al. Robustness of patient positioning for interfractional error in carbon ion radiotherapy for stage I lung cancer: bone matching versus tumor matching. Radiother Oncol 2017;129:95–100.
[14] Moriya S, Tachibana H, Hotta K, et al. Feasibility of dynamic adaptive passive scattering proton therapy with computed tomography image guidance in the lung. Med Phys 2017;44:4474–81.
[15] Houweling AC, Fukata K, Kubota Y, et al. The impact of interfractional anatomical changes on the accumulated dose in carbon ion therapy of pancreatic cancer patients. Radiother Oncol 2016;119:319–25.
[16] Kubota Y, Katoh H, Shibuya K, et al. comparison between bone matching and marker matching for evaluation of intra- and inter-fractional changes in accumulated of carbon ion radiotherapy for hepatocellular carcinoma. Radiother Oncol 2019;137:77–82.
[17] Kanematsu N. Dose calculation algorithm of fast fine-heterogeneity correction for heavy charged particle radiotherapy. Phys Med 2011;27:97–102.
[18] Ohno T. Particle radiotherapy with carbon ion beams. EPMA J 2013;4:9.
[19] Jaffray DA. Image-guided radiotherapy: from current concept to future perspectives. Nat Rev Clin Oncol 2012;9:688–99.
[20] Li Y, Kubota Y, Tashiro M, et al. Value of three-dimensional imaging systems for image-guided carbon ion radiotherapy. Cancers 2019;11:E297.
[21] Starkschall G, Balter P, Britton K, et al. Interfractional reproducibility of lung tumor location using various methods of respiratory motion mitigation. Int J Radiat Oncol Biol Phys 2011;79:596–601.

[22] Mampuya WA, Nakamura M, Matsuo Y, et al. Interfraction variation in lung tumor position with abdominal compression during stereotactic body radiotherapy. Med Phys 2013;40:091718.
[23] Kestin L, Grills I, Guckenberger M, et al. Dose–response relationship with clinical outcome for lung stereotactic body radiotherapy (SBRT) delivered via online image guidance. Radiother Oncol 2014;110:499–504.
[24] Kanemoto A, Okumura T, Ishikawa H, et al. Outcomes and prognostic factors for recurrence after high-dose proton beam therapy for centrally and peripherally located stage I non-small-cell lung cancer. Clin Lung Cancer 2014;15:e7–e12.
[25] Takao S, Miyamoto N, Matsuura T, et al. Intrafractional baseline shift or drift of lung tumor motion during gated radiation therapy with a real-time tumor-tracking system. Int J Radiat Oncol Biol Phys 2016;94:172–80.
[26] Trnková P, Knäusl B, Actis O, et al. Clinical implementations of 4D pencil beam scanned particle therapy: report on the 4D treatment planning workshop 2016 and 2017. Phys Med 2018;54:121–30.
[27] Knopf AC, Stützer K, Richter C, et al. Required transition from research to clinical application: report on the 4D treatment planning workshops 2014 and 2015. Phys Med 2016;32:874–82.
[28] Knopf A, Nill S, Yohannes I, et al. Challenges of radiotherapy: report on the 4D treatment planning workshop 2013. Phys. Med 2014;30:809–15.
[29] Moriya S, Tachibana H, Kitamura N, et al. Dose warping performance in deformable image registration in lung. Phys Med 2017;37:16–23.
[30] Kubota Y, Okamoto M, Li Y, et al. Evaluation of intensity- and contour-based deformable image registration accuracy in pancreatic cancer patients. Cancers 2019;11:E1447.
[31] Grassberger C, Dowdell S, Lomax A, et al. Motion interplay as a function of patient parameters and spot size in spot scanning proton therapy for lung cancer. Int J Radiat Oncol Biol Phys 2013;86:380–6.
[32] Mori S, Knopf AC, Umegaki K, et al. Motion management in particle therapy. Med Phys 2018;45:e994–e1010.